Differential Scanning Calorimetry Studies on High- and Low-Density Annealed and Irradiated Polyethylenes: Influence of Aging

A. Vallés-Lluch, L. Contat-Rodrigo, A. Ribes-Greus

Department of Applied Thermodynamics, Escuela Técnica Superior de Ingenieros Industriales de Valencia, P.O. Box 22012, 46071 Valencia, Spain

Received 15 July 2002; accepted 21 November 2002

ABSTRACT: The effect of γ-radiation, followed by 10 years storage at ambient conditions, on the thermal behavior of different types of high- and low-density commercial polyethylenes was studied. First, samples were annealed to improve the crystalline content. Next, they were irradiated, after which fusion endotherms, melting temperatures, crystallinity indices, and lamellar thicknesses were obtained by differential scanning calorimetry (DSC). The change in the thermal parameters for the first and second meltings were related to the absorbed doses. Afterward, the samples were stored at ambient conditions for 10 years and then scanned again by DSC to assess the influence of aging on previously irradiated samples. The results showed that the changes on the morphological structure undergone by the samples with the storage time were highly dependent on the polyethylene type and the absorbed radiation dose. The high-density polyethylene was the most sensitive to radiation and storage, whereas the low-density polyethylene with the lowest molecular weight and the highest degree of branching was the least affected. In general, the changes observed during irradiation can be explained in terms of an increase of imperfections and chain scissions. The storage can be understood as a slow crystallization process at low radiation doses, and as a decrease of the crystalline structure at high doses. © 2003 Wiley Periodicals, Inc. J Appl Polym Sci 89: 3260–3271, 2003

Key words: polyethylene (PE); irradiation; annealing; aging; differential scanning calorimetry (DSC)

INTRODUCTION

Polymers are in some cases used in environments where they may be exposed to high-energy radiation, for instance, nuclear power plants, radiation equipment, particle-physics generators, and mainly in sterilization systems (medical equipment, hospital clothing, foodstuffs packaging, etc.). Ionizing radiation is capable of producing chemical and morphological changes that may either deteriorate or improve certain properties to fit a specific desired application.[1]

Over the years, the effects of high-energy radiation on polyethylene have been extensively studied,[2–20] but they are still subject to debate because of the variety of interpretations proposed by different authors. Irradiation causes important changes that often occur simultaneously, that is, crosslinking processes at chain ends, unsaturations, and main chain scissions, for example, and consequently changes on the melting behavior and crystallinity. Many factors such as the polyethylene type, the absorbed dose, irradiation conditions as the temperature, the dose rate, and the irradiation atmosphere largely influence these processes.

Furthermore, the crystalline morphology is another key issue to consider. The thermal treatment promotes reorganization in the crystalline zone, thus accelerating the radiation effects.[12] For this reason, samples of high- and low-density polyethylenes were submitted to a thermal treatment before irradiation.

The purpose of this work was to study the effect of different doses of ionizing radiation from a γ-source on the melting behavior of high- and low-density polyethylenes by means of differential scanning calorimetry (DSC). This technique has been proposed by many authors[6–11,14–16,20] as a suitable analytical tool for these studies when the measurement is performed at high enough heating rates (10–20°C/min) given that at such heating rates reorganization effects during the scan are minimal.

On the other hand, few results[6,8,13] have been reported on the effects of storage on previously irradiated polyethylenes. Thus, in this work, samples of low- and high-density irradiated polyethylenes were stored for 10 years at ambient conditions and afterward scanned by DSC to investigate their morphological changes.

EXPERIMENTAL

Materials

Three different types of polyethylenes were supplied by Dow Chemical Ibérica S.A. (Tarragona, Spain). The com-

Correspondence to: A. Ribes-Greus (aribes@ter.upv.es).

Contract grant sponsor: Ministerio de Ciencia y Tecnología of Spain; contract grant number: PPQ2001-2764-C03-01.

© 2003 Wiley Periodicals, Inc.

TABLE I
Variation of Concentration of Carbonyl Groups: Aldehyde (CHO) and Ketone (CO), and Functional Groups: *trans*-Vinylene (CH=CH), Vinyl ($CH=CH_2$), and Vinylidene ($C=CH_2$), for HDPE 10062, LDPE 710, and LDPE 980, Related to the Radiation Dose

		Functional group				
Sample	Radiation dose (Mrad)	Aldehyde CHO	Ketone CO	*trans*-Vinylene CH=CH	Vinyl $CH=CH_2$	Vinylidene $C=CH_2$
HDPE 10062	0	0.010	0.012	0.000	0.536	0.034
	2	0.298	0.436	0.077	0.393	0.035
	20	0.720	1.388	0.273	0.549	0.022
	100	0.426	0.345	0.583	0.020	0.031
LDPE 710	0	0.174	0.322	0.037	0.092	0.200
	2	0.269	0.406	0.085	0.083	0.186
	20	0.505	0.574	0.388	0.081	0.100
	100	0.561	0.880	1.114	0.095	0.100
LDPE 980	0	0.131	0.242	0.043	0.091	0.210
	2	0.207	0.391	0.078	0.086	0.162
	20	0.339	0.608	0.357	0.084	0.108
	100	0.637	0.957	1.095	0.102	0.105

mercial labels of the polyethylenes are as follows: high-density polyethylene, HDPE 10062 ($M_n = 18.8 \times 10^3$, $M_w = 62.7 \times 10^3$, $-CH_3/1000CH_2 = 0.21$); low-density polyethylenes, LDPE 710 ($M_n = 7.53 \times 10^3$, $M_w = 47.6 \times 10^3$, $-CH_3/1000CH_2 = 1.90$); and LDPE 980 ($M_n = 6.22 \times 10^3$, $M_w = 46.8 \times 10^3$, $-CH_3/1000CH_2 = 2.50$).

Preparation and thermal treatment of samples

Thermal history was as follows: first, all the samples were prepared from pellets by compression molding in an M Carver press, at 170°C for 10 min, at 14 bar. The thickness of the samples was about 1 mm. The samples were then cooled at 20°C in the molding press. Next, they were annealed in a forced ventilation oven at 104.6 ± 0.1°C under air atmosphere, for 65 h. Finally, the samples were quenched in a water-ice bath at 0°C, to ensure that all the samples received the same thermal history.

Irradiation treatment

After annealing, the irradiation was carried out at a constant temperature of 20°C under air atmosphere with γ-rays from a ^{60}Co source at the same dose rate of 1.4×10^{-4} Mrad/s. The total doses were 2, 20, and 100 Mrad, respectively, for the different samples. Unirradiated samples were kept to be used as control materials.

Spectrometry measurements

All samples were scanned in an infrared spectrophotometer Nicolet 510 FTIR (Nicolet Instruments, Madison, WI) in the reflection (ATR) mode. For each measurement 100 scans were averaged at a resolution of 4 cm^{-1} from 400 to 4000 cm^{-1}.

Storage

A series of samples (denoted as aged samples) were stored at room temperature for 10 years, for comparison with the unaged samples.

DSC measurements

DSC measurements were performed for both unaged and aged samples on a Perkin–Elmer DSC-4 calorimeter (Perkin Elmer Cetus Instruments, Norwalk, CT), under nitrogen atmosphere, and previously calibrated with indium standard. About 6–7 mg of sample were accurately weighed in a standard aluminum pan. The pans were sealed, pierced, and heated from 0 to 180°C at a heating rate of 20°C/min in a first scan. Afterward the samples were cooled to 0°C at a cooling rate of 40°C/min and heated again to 180°C at 20°C/min in a second scan.

Measurements were repeated to ensure errors of no more than ±0.1°C for melting temperatures and ±0.5% for crystalline contents.

RESULTS AND DISCUSSION

Spectrometry measurements

The chemical structure of the unaged samples was studied by determination of the functional groups aldehyde, ketone, vinyl, vinylidene, and *trans*-vinylene. The number of functional groups was determined by the analysis of the absorption peaks of the spectra: at 1730 cm^{-1} for the aldehyde group, at 1713 cm^{-1} for the ketone group, at 965 cm^{-1} for the *trans*-vinylene group, at 909 cm^{-1} for the vinyl group, and at 888 cm^{-1} for the vinylidene group. The equations used for this purpose were those proposed by Sato,[21]

as in previous works.[22,23] Table I displays the results obtained for the different functional groups.

In the low-density polyethylenes the concentration of the vinylidene groups decreases, whereas the number of imperfections in molecular chains (*trans*-vinylene, aldehyde, and ketone groups) increases with increasing radiation doses.

In the high-density polyethylene, the number of vinyl groups decreases with increasing absorbed doses. The concentration of carbonyl groups (aldehyde and ketone) increases at low doses (0–20 Mrad), whereas it strongly decreases at higher doses (20–100 Mrad). The number of *trans*-vinylene groups increases, but not as much as in the low-density polyethylenes.

The obtained results suggest that irradiation increases the number of imperfections in molecular chains. Katsumura[17] attributed the rapid disappearance of the vinyl and vinylidene groups to the addition to the double bonds of initial radicals produced during irradiation, which leads to crosslinking. Moreover, carbonyl groups have been reported in the literature[6–8,13] to produce crosslinkings and/or chain scissions, of which chain scissions are more likely to occur in an oxygen atmosphere.[10] The fact that the number of carbonyl groups decreases in the HDPE when submitted to high radiation doses could be understood from the basis that a significant number of chain scissions likely have been formed in HDPE.

DSC measurements

Calorimetric analysis was performed to study the morphological changes undergone by the samples during the irradiation process, and also after the aging test.

Two scans were carried out for all the samples. The first scan brings forward the direct effect of irradiation (and aging, in the case of aged samples) on the crystalline structure of the samples. The second scan reflects the realignment of the chains after chain scissions or the impediments in crystal growth caused by noncrystallizable defects in the polymeric chains.

Figures 1, 2, and 3 show the DSC thermograms for the HDPE 10062, LDPE 710, and LDPE 980 (both unaged and aged) samples, respectively, unirradiated and irradiated with 100-Mrad radiation dose, for the first and second scans. The thermograms do not show significant differences between the unirradiated samples and the respective irradiated ones.

In general, the storage produces a slight shift of the thermograms in the temperature axis in the three polyethylenes. When samples were scanned for a second time, the thermograms shifted slightly to lower temperatures and the curves appeared more homogeneous in shape. The effect of storage seemed to be more noticeable in the second scan, for the HDPE 10062 and LDPE 710 samples. However, in the thermograms of the LDPE 980 samples, hardly any differences can be observed between the unaged and aged samples in the second scan.

To analyze the morphological changes in more detail, the melting temperature, the crystalline content, and the lamellar thickness distribution were calculated.

Melting temperature

The melting temperature (T_m) was determined in all samples for both scans directly from the thermograms as the temperature of the main endotherm.

The melting temperatures for LDPE 980, both unaged and aged samples, related to the increasing radiation doses are plotted in Figure 4 for the first and second scans. In the second scan, the T_m values are always lower than those in the first scan. This effect was observed for the three polyethylenes under study.

To better observe the effect of storage, the evolution of T_m for the first scan, for both the unaged and the aged samples of the three polyethylenes, is shown in Figure 5. For the unaged samples, the same tendency was observed for the three polyethylenes. At low radiation doses the melting temperatures decrease, but for higher doses, they level off or increase.

In these unaged samples, the decrease in the melting points at low doses can be attributed to the increase in the number of molecular defects (ketone, aldehyde, and *trans*-vinylidene groups). All these molecular defects hinder the crystallization process.[10] When the absorbed doses increase, two competitive processes might occur: on one hand, the formation of imperfections and crosslinkings in the polymeric chains, and on the other hand, chain scissions yielding radicals that do not recombine. The rupture of the bonds allows polymer chains to increase their lamellar thicknesses, consequently increasing the melting temperatures. The molecular structure of each polyethylene will promote one process over the other. The slight increase in the melting temperature in the lineal polyethylene (HDPE 10062) and in the low-density, less-branched polyethylene (LDPE 710) could indicate that scission is slightly predominant over crosslinking.

By contrast, when comparing the evolution of the melting temperatures of the aged samples with that of the unaged ones, interesting features related to the type of polyethylene are noted. For low radiation doses, the melting temperatures of the aged samples are higher than those of the respective unaged samples. However, at high radiation doses, HDPE 10062 and LDPE 710 aged samples exhibit a different trend than that of the corresponding unaged samples, reaching lower values, whereas the LDPE 980 aged samples maintained the same relationship between the melting temperatures and the radiation doses as that of the unaged ones.

The fact that the melting temperatures of the aged samples irradiated with low radiation doses are

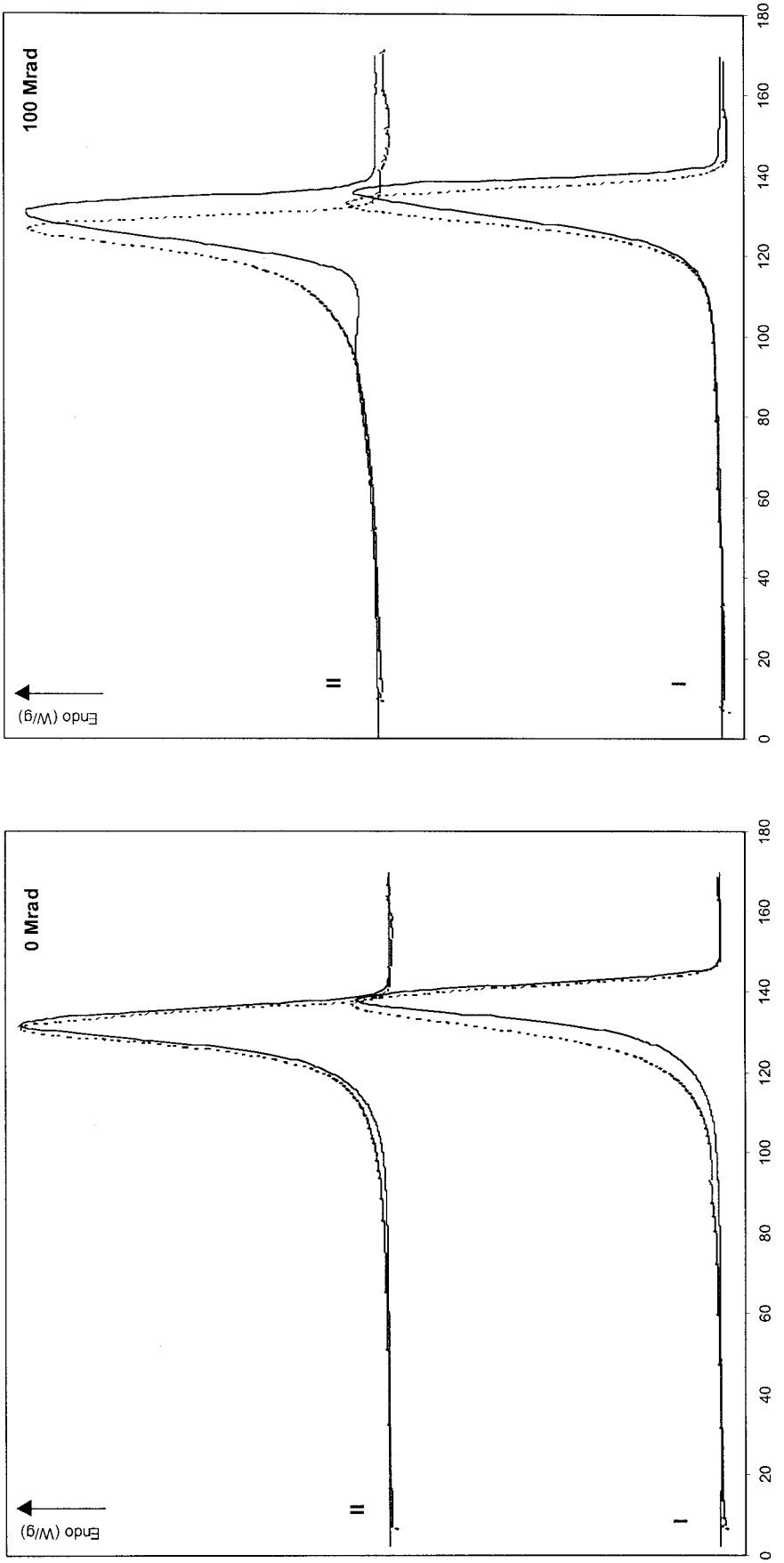

Figure 1 DSC thermograms for the HDPE 10062, (—) unaged and (- - -) aged samples, irradiated with 0 and 100 Mrad radiation doses, for the (**I**) first and (**II**) second scans.

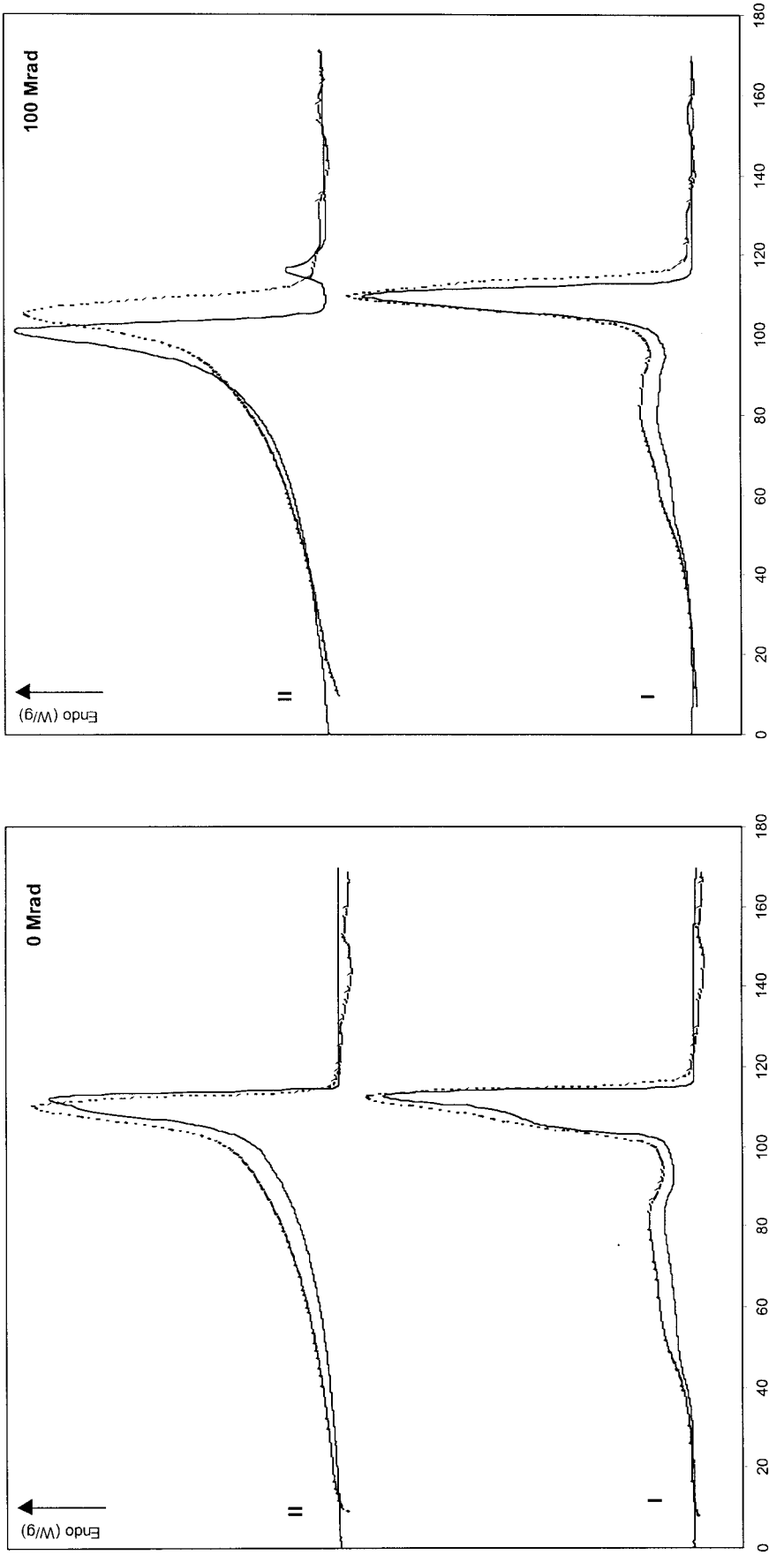

Figure 2 DSC thermograms for the LDPE 710, (—) unaged and (- - -) aged samples, irradiated with 0 and 100 Mrad radiation doses, for the (**I**) first and (**II**) second scans.

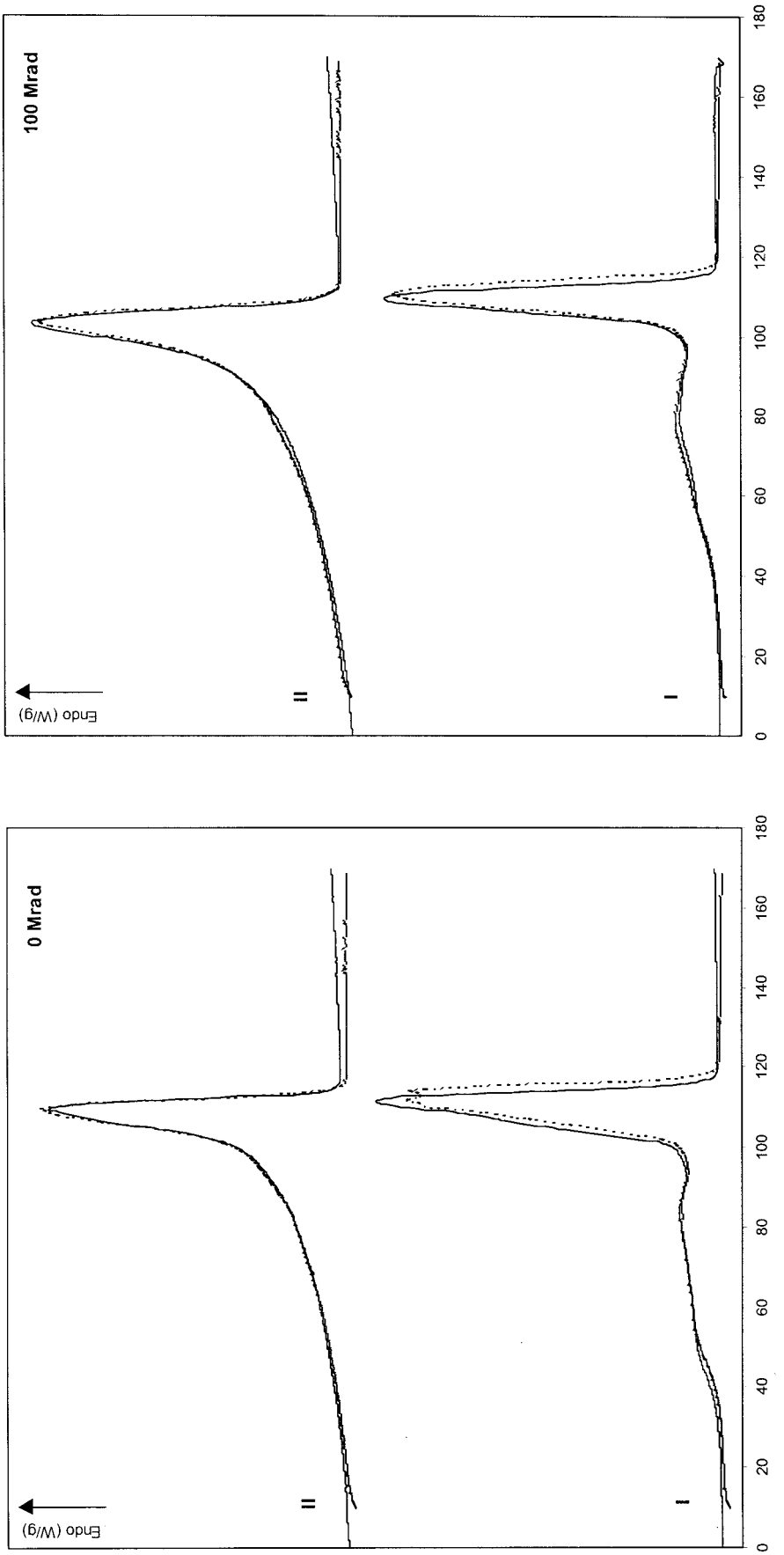

Figure 3 DSC thermograms for the LDPE 980, (—) unaged and (- - -) aged samples, irradiated with 0 and 100 Mrad radiation doses, for the (**I**) first and (**II**) second scans.

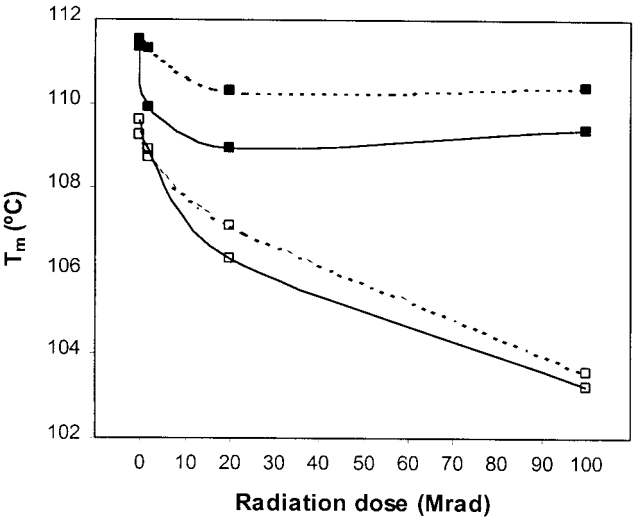

Figure 4 Melting temperatures for LDPE 980, both (—) unaged and (- - -) aged samples, for the (■) first and (□) second scans.

higher than those corresponding to the unaged samples could be explained in terms of a slow crystallization process taking place during storage. However, at higher absorbed doses, carbonyl groups produced by irradiation might lead to chain scissions at a greater scale, which could deteriorate the crystalline structure.

To confirm these hypotheses, determination of the crystalline contents and the lamellar thickness distributions was carried out.

Crystalline content

The crystalline content (X) was calculated for each sample as $X = (H_m - H_c)/\Delta H_m^0$, where H_m and H_c are the enthalpies per mass unit in the melt and crystalline states, respectively. Their difference is determined from the area of the endothermic peak ΔH_m, given directly by the DSC instrument. The melting enthalpy ΔH_m^0 of an infinite crystal per mass unit is 288 J/g.[24]

The crystalline content related to the absorbed radiation doses for LDPE 980 both unaged and aged samples is represented in Figure 6 for the first and second scans. A decrease in the crystalline content may be observed in the second scan compared to those of the first scan, for both unaged and aged samples. This was observed for the three polyethylenes under study.

The crystalline content of the first scan for the unaged and aged samples of the three types of polyethylenes is displayed in Figure 7. As expected, the crystallinity of the high-density polyethylene is much higher than that of the low-density polyethylenes. For the unaged samples, an initial decrease in the crystalline content with increasing radiation dose is observed. At higher doses, the crystalline content remains almost practically constant in the low-density

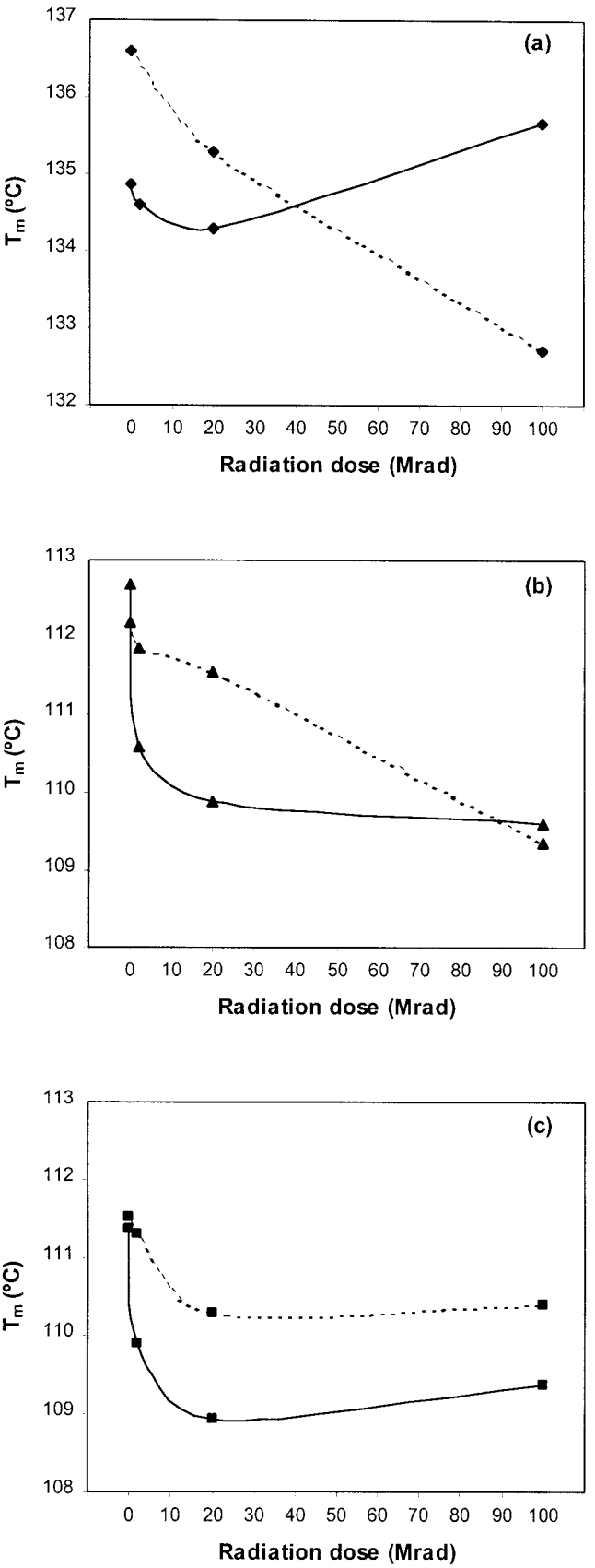

Figure 5 Melting temperatures for the first scan, for (a) HDPE 10062, (b) LDPE 710, and (c) LDPE 980 (—) unaged and (- - -) aged samples.

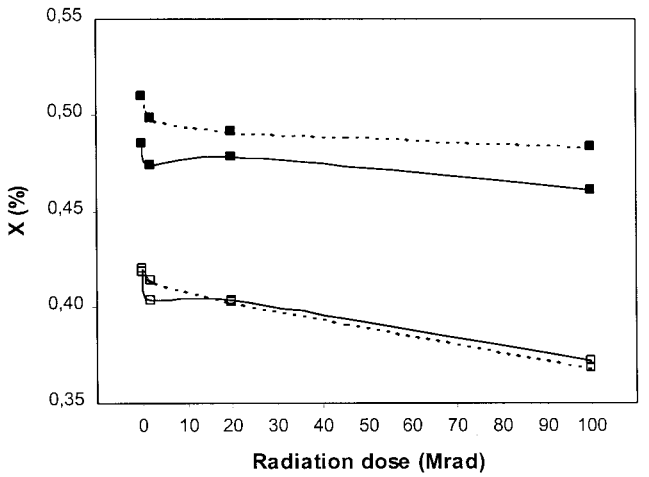

Figure 6 Crystalline contents for LDPE 980 both (—) unaged and (- - -) aged samples, for the (■) first and (□) second scan.

polyethylenes, whereas it increases in the high-density one.

Furthermore, the crystalline content for the aged samples is in all cases higher than that of the unaged samples. As proposed above, the chains previously broken by irradiation seem to reorganize and crystallize during storage, thus increasing the total crystalline index compared to that of the unaged samples. It agrees with Hawkins,[25] who suggests that the crystalline content in a semicrystalline polymer is conditioned by the amorphous phase that restricts the crystallization process. A scission of the molecules of the amorphous regions allows the crystallization to proceed to a greater extent.

Lamellar thickness distribution

The lamellar thickness distribution was determined for each sample according to the method proposed by Eder,[26] who assumes that the rate of heat consumption at a given temperature is directly proportional to the fraction of lamellae whose thickness is given from the Thomson equation, from which it is deduced:

$$l = \frac{2\sigma_e}{\Delta H_v^0\left(1 - \frac{T_m}{T_m^0}\right)}$$

where T_m is the observed melting point of lamellae of thickness l, $T_m^0$is the equilibrium melting point of an infinite crystal, σ_e is the surface free energy of the basal plane, and ΔH_v^0 is the enthalpy of fusion per unit volume. Considering the values of these parameters for polyethylene as $T_m^0 = 414.2$ K,[27] $\sigma_e = 60.9 \times 10^{-3}$ J/m^2,[26] and $\Delta H_v^0 = 2.88 \times 10^8$ J/m^3,[26] the lamellar thickness corresponding to each temperature can be calculated.

Figures 8, 9, and 10 show the lamellar thickness distributions for the HDPE 10062, LDPE 710, and LDPE 980 samples, respectively, unirradiated and irradiated with 100 Mrad radiation dose, for the first

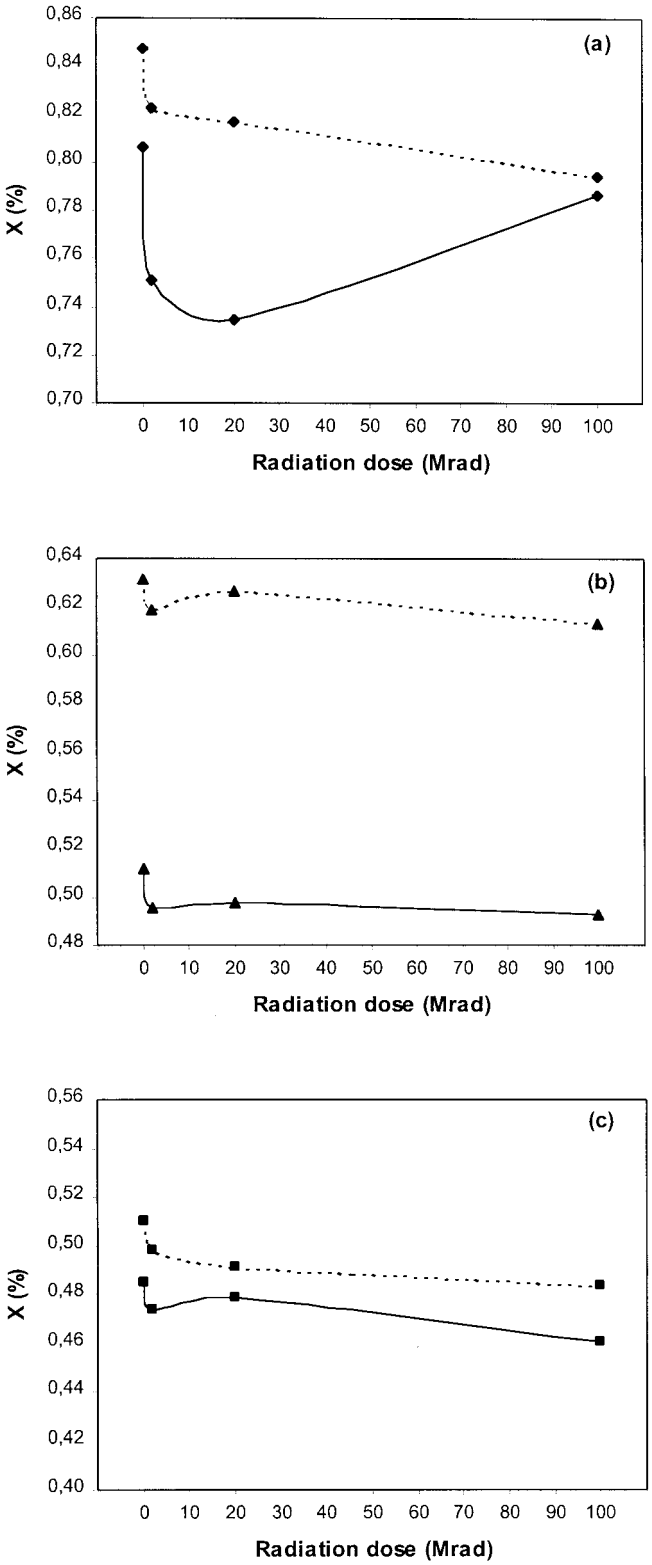

Figure 7 Crystalline contents for the first scan for (a) HDPE 10062, (b) LDPE 710, and (c) LDPE 980 (—) unaged and (- - -) aged samples.

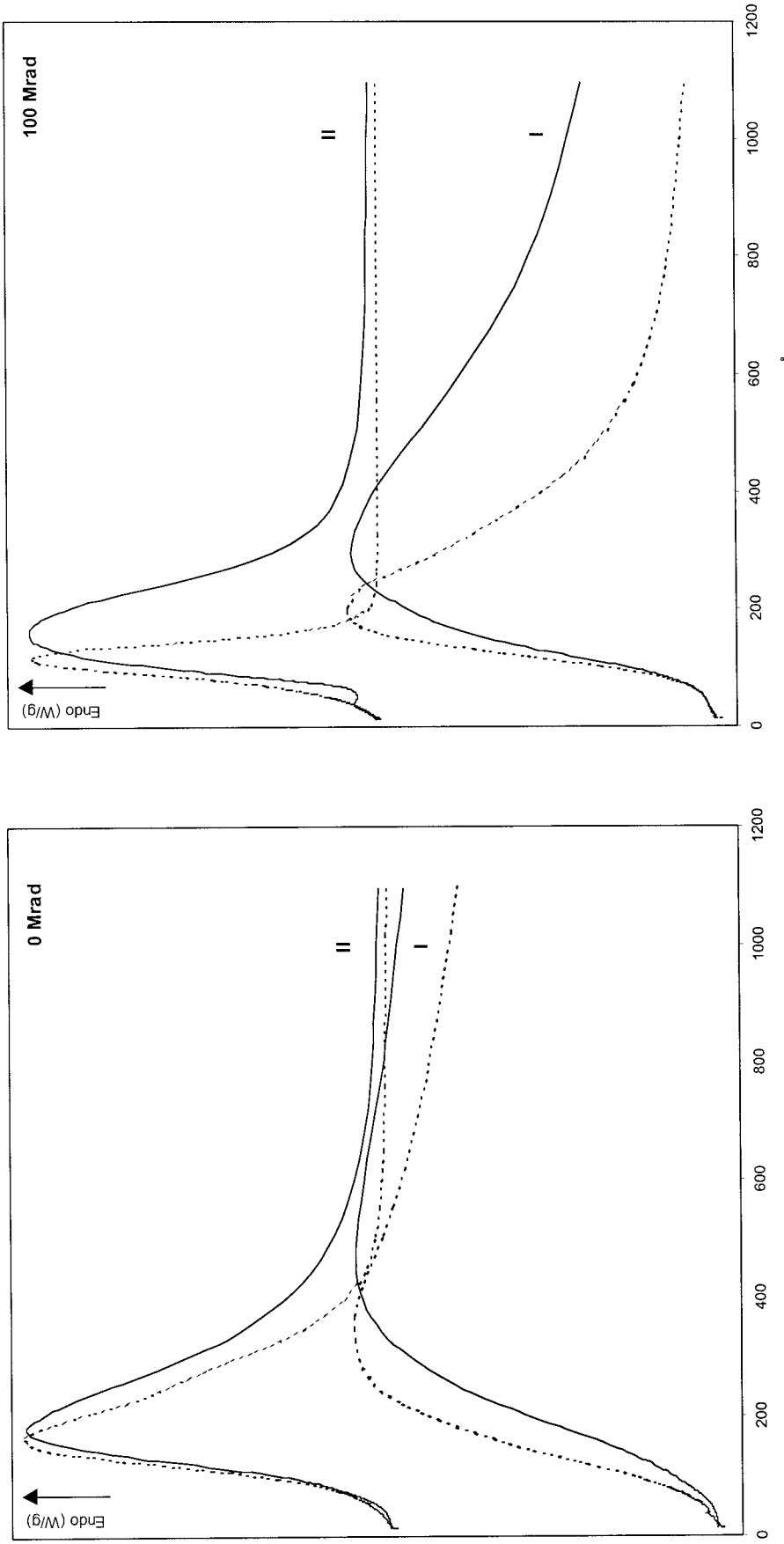

Figure 8 Distribution of lamellar thickness for the HDPE 10062, (—) unaged and (- - -) aged samples, irradiated with 0 and 100 Mrad radiation doses, for the (**I**) first and (**II**) second scans.

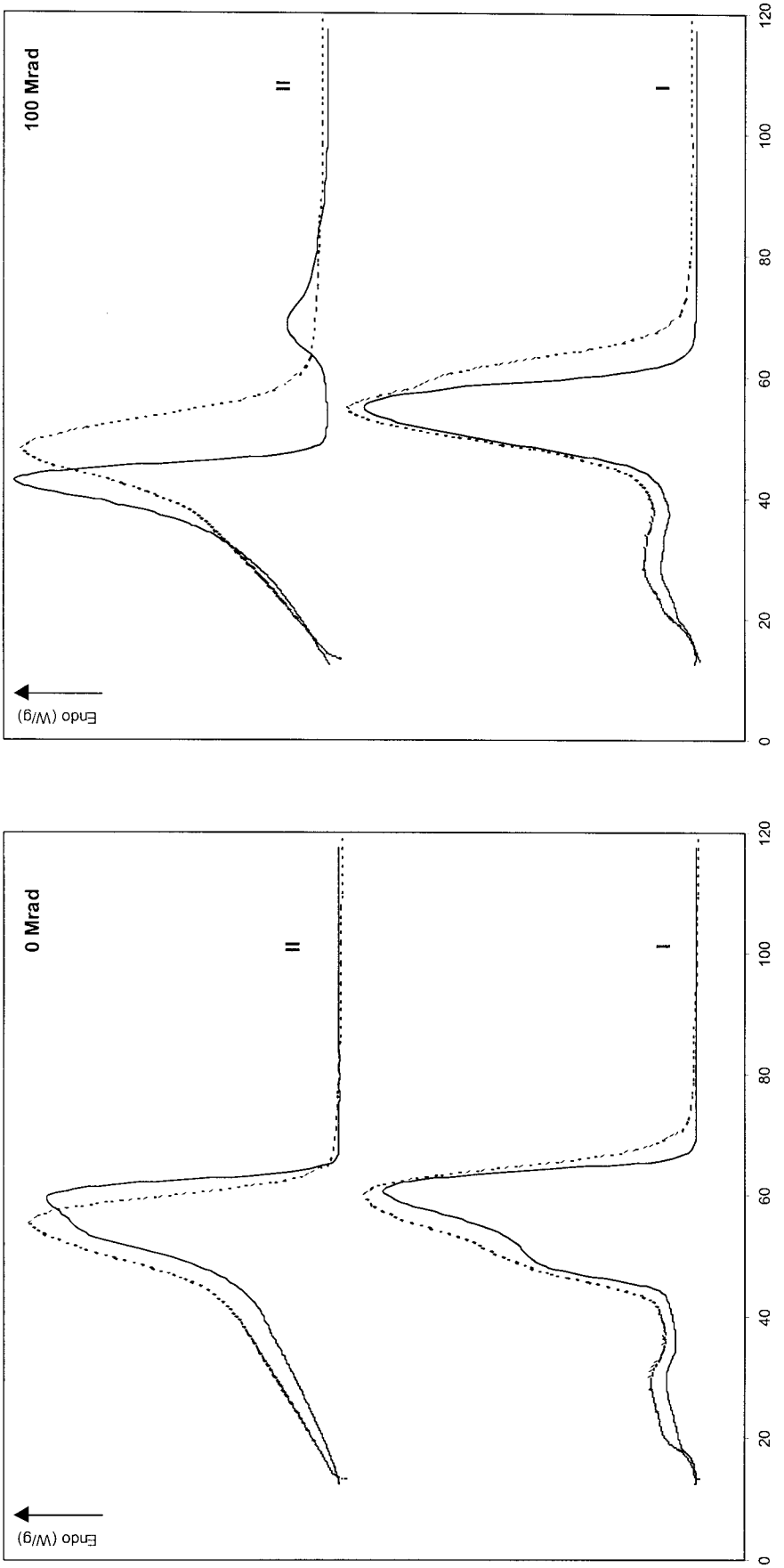

Figure 9 Distribution of lamellar thickness for the LDPE 710, (—) unaged and (- - -) aged samples, irradiated with 0 and 100 Mrad radiation doses, for the (**I**) first and (**II**) second scans.

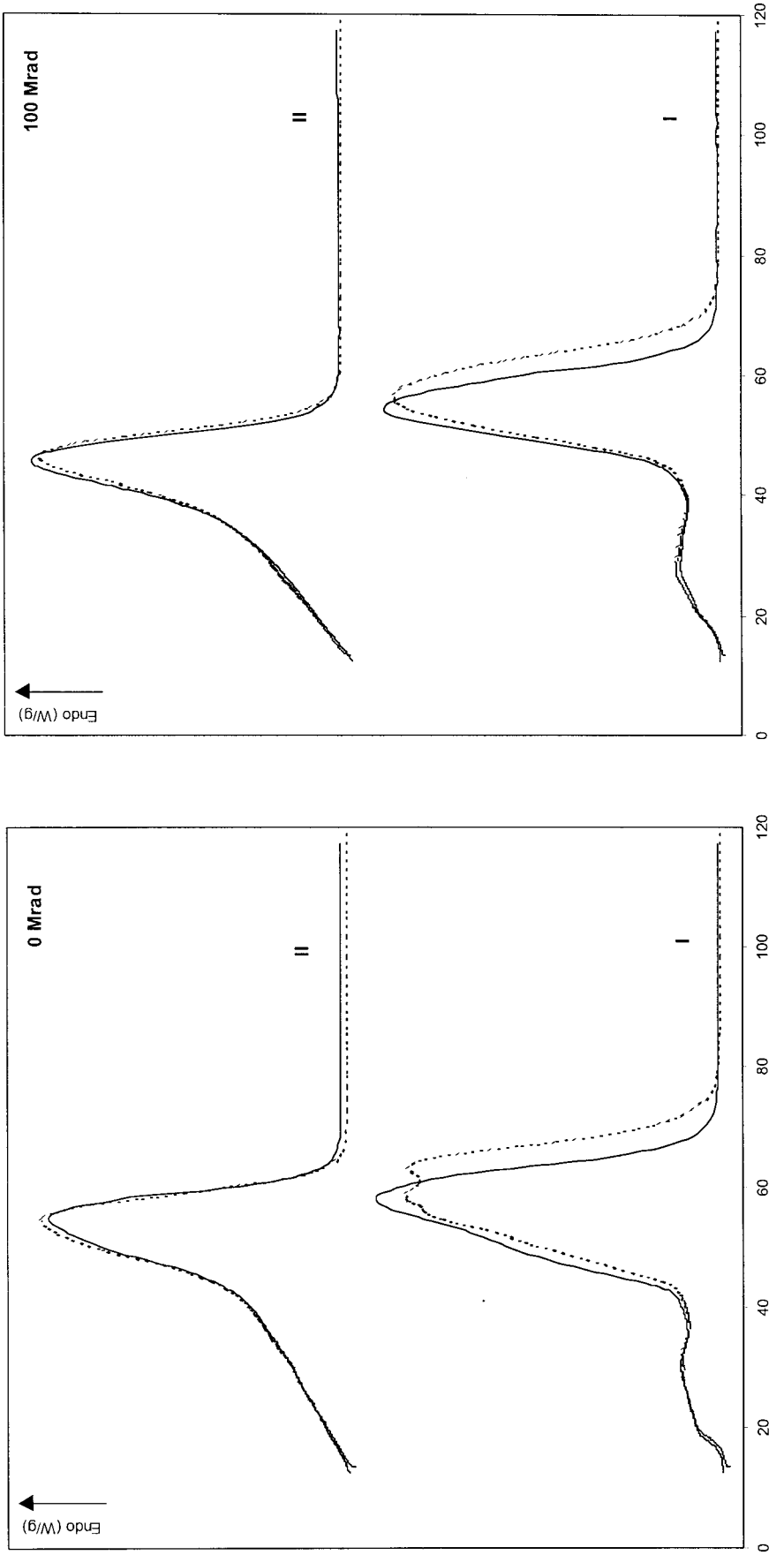

Figure 10 Distribution of lamellar thickness for the LDPE 980, (—) unaged and (- - -) aged samples, irradiated with 0 and 100 Mrad radiation doses, for the (**I**) first and (**II**) second scans.

and second scans. In general, the irradiated samples display slightly narrower distributions compared to those of the unirradiated ones.

The distributions for the low-density polyethylene samples consist of a main endotherm centered about 50–60 Å, and a small shoulder attributed to the smallest crystallites. The distributions resulting from the second scan are slightly shifted to lower thicknesses compared to those of the first scan, and the shape of the curves becomes more homogeneous as the small shoulders at low thicknesses disappear. The storage causes a slight broadening in the LDPE 710 samples, as well as a slight shift of the distributions in the temperature axis, although these effects are hardly noticeable in the LDPE 980 samples, whose molecular weight is the lowest and the degree of branching is the highest.

The thicknesses of the lamellae are much higher for the high-density polyethylene than those of the low-density polyethylenes, as expected, and the shape of the curves is significantly different. With the second scan the curves for high-density polyethylene shift to lower thicknesses and the distributions of crystallite sizes are narrower, compared to the curves for the first scan. The storage still narrows and shifts the distribution to a greater degree to the smaller crystallites, thus demonstrating a more noticeable effect in the second scan.

The most probable crystallite thickness (l_{max}) was calculated in each case as the crystallite thickness of the maximum of the lamellar thickness distribution. The evolution of l_{max} with the absorbed radiation dose is totally analogous to that obtained for the melting temperature, as expected. Again, the high-density polyethylene was found to be more sensitive to γ-radiation in terms of l_{max} with respect to the low-density polyethylenes, as occurred with the melting points and the total crystalline content.

CONCLUSIONS

These morphological changes undergone by the samples during irradiation can be explained in terms of an increase of imperfections and chain scissions.

Thus, for all the studied (high- and low-density) unaged polyethylenes, low radiation doses produce a decrease in the melting temperature, crystalline content, and most probably crystallite thickness because of an increase in the number of molecular defects (crosslinkings, carbonyl groups, and unsaturations) in the polymer chains. At high doses, the rupture of the carbonyl groups in the high-density polyethylene seems to lead to chain scissions. This allows the recrystallization of polymer chains, thus increasing the melting temperature and the crystalline content.

The aging process seems to involve a recrystallization of the broken chains for all the polyethylenes when they are irradiated with low doses. At higher radiation doses, the aging effect depends on the chemical structure. In the low-density polyethylenes, the molecular defects limit the crystallization process. In the high-density polyethylene, the broken chains might cause a deterioration in the crystalline structure.

The high-density polyethylene (HDPE 10062) displays the most significant morphological changes, whereas the low-density polyethylene with the lowest molecular weight and the highest degree of branching (LDPE 980) was found to best resist the irradiation treatment and the following storage.

The authors are grateful for the financial support received for this work from the Ministerio de Ciencia y Tecnología of Spain by the project PPQ2001-2764-C03-01.

References

1. Scott, G. Mechanisms of Polymer Degradation and Stabilisation; Elsevier Science Publishers: Essex, 1990.
2. Charlesby, A. Atomic Radiation and Polymers; Pergamon Press: Oxford, 1960.
3. Dole, M. The Radiation Chemistry of Macromolecules; Academic Press: New York, 1972.
4. Patel, G. N.; Keller, H. H. J Polym Sci Part B: Polym Phys 1975, 13, 303.
5. Ahmad, S. R.; Charlesby, A. Int Radiat Phys Chem 1976, 8, 585.
6. Batheja, S. K. Polymer 1982, 23, 654.
7. Bhateja, S. K. J Macromol Sci Phys 1983, B22, 159.
8. Bhateja, S. K. J Appl Polym Sci 1983, 28, 861.
9. Zoepfl, F. J.; Markovic, V.; Silverman, J. J Polym Sci Part A: Polym Chem 1984, 22, 2017.
10. Shinde, A.; Salovey, R. J Polym Sci Part B: Polym Phys 1985, 23, 1681.
11. Aslanian, V. M.; Vardanian, V. I.; Avetisian, M. H.; Felekian, S. S.; Ayvasian, S. R. Polymer 1987, 28, 755.
12. Geetha, R.; Torikai, A.; Yoshida, S.; Nagaya, S.; Shirakawa, H.; Fueki, K. Polym Degrad Stab 1988, 23, 91.
13. Birkinshaw, C.; Buggy, M.; Daly, S.; O'Neill, M. Polym Degrad Stab 1988, 22, 285.
14. Ribes-Greus, A.; Díaz-Calleja, R. J Appl Polym Sci 1989, 37, 2549.
15. Sáenz de Juano-Arbona, V.; Ribes-Greus, A.; Díaz-Calleja, R.; Alcaina-Miranda, I.; Del Hierro-Navarro, P.; Sanz-Box, C.; Trijueque-Monge, J. J Non-Cryst Solids 1994, 172–174, 1072.
16. Kačarević-Popović, Z.; Kostoski, D.; Stojanović, Z.; Doković, V. Polym Degrad Stab 1997, 56, 227.
17. Wu, G.; Katsumura, Y.; Kudoh, H.; Morita, Y.; Seguchi, T. J Polym Sci Part A: Polym Chem 1999, 37, 1541.
18. Yu, Y.-J.; Shen, F.-W.; Mckellop, H. A.; Salovey, R. J Polym Sci Part A: Polym Chem 1999, 37, 3309.
19. Abou Zeid, H. M.; Ali, Z. I.; Abdel Maksoud, T. M.; Khafagy, R. M. J Appl Polym Sci 2000, 75, 179.
20. Badr, Y.; Ali, Z. I.; Zahran, A. H.; Khafagy, R. M. Polym Int 2000, 49, 1555.
21. Sato, Y.; Yashiro, T. J Appl Polym Sci 1978, 22, 2141.
22. Ribes-Greus, A.; Díaz-Calleja, R. J Appl Polym Sci 1989, 38, 1127.
23. Ribes-Greus, A.; Díaz-Calleja, R. J Appl Polym Sci 1989, 34, 2819.
24. Wunderlich, B. Macromolecular Physics; Academic Press: New York, 1973; Vol. 1, p. 388.
25. Hawkins, W. Polymer Degradation and Stabilization; Springer-Verlag: Berlin, 1984.
26. Wlochowicz, A.; Eder, M. Polymer 1984, 25, 1268.
27. Turi, E. A. Thermal Characterization of Polymeric Materials; Academic Press: New York, 1997; Vol. 1, p. 372.